sustainability

MDPI

Article

Impacts of Thermal Power Industry Emissions on Air Quality in China

Xiuyong Zhao [1], Wenxin Tian [1] and Dongsheng Chen [2,*]

[1] State Key Laboratory of Low-Carbon Smart Coal-Fired Power Generation and Ultra-Clean Emission, China Energy Science and Technology Research Institute Co., Ltd., Nanjing 210023, China; zhxiuyong@126.com (X.Z.); twxtim@gmail.com (W.T.)
[2] Key Laboratory of Beijing on Regional Air Pollution Control, Beijing University of Technology, Beijing 100124, China
* Correspondence: dschen@bjut.edu.cn; Tel.: +86-10-6739-1659

Abstract: Power plants remain major contributors to air pollution, and while their impact on air quality and atmospheric chemistry have been extensively studied, there are still uncertainties in quantifying their precise contributions to $PM_{2.5}$ and O_3 formation under varying environmental conditions. This study employs the WRF/CMAQ modeling system to quantify the impact of power plant emissions on PM2.5 and O_3 levels across eastern China in June 2019. We investigate the spatial and temporal patterns of pollutant formation, analyze contributions to secondary PM2.5 components, and assess process-specific influences on O_3 concentrations. Results show that power plant emissions contribute up to 2.5–3.0 μg m^{-3} to $PM_{2.5}$ levels in central and eastern regions, with lower impacts in coastal and southern areas. O_3 contributions exhibit a more complex pattern, ranging from −4 to +4 ppb, reflecting regional variations in NOx saturation. Among secondary $PM_{2.5}$ components, nitrate formation is most significantly influenced by power plant emissions, emphasizing the critical role of NOx. Diurnal O_3 patterns reveal a transition from widespread morning suppression to afternoon enhancement, particularly in southern regions. Process analysis indicates that vertical transport is the primary mechanism enhancing surface O_3 from power plant emissions, while dry deposition acts as the main removal process. This comprehensive assessment provides crucial insights for developing targeted air quality management strategies, highlighting the need for region-specific approaches and prioritized NOx emission controls in the power sector. Our findings contribute to a deeper understanding of the complex relationships between power plant emissions and regional air quality, offering a foundation for more effective pollution mitigation policies.

Keywords: thermal power industry; $PM_{2.5}$; O_3; WRF/CMAQ

Academic Editor: Giouli Mihalakakou

Received: 16 October 2024
Revised: 12 December 2024
Accepted: 2 January 2025
Published: 8 January 2025

Citation: Zhao, X.; Tian, W.; Chen, D. Impacts of Thermal Power Industry Emissions on Air Quality in China. *Sustainability* **2025**, *17*, 441. https://doi.org/10.3390/su17020441

1. Introduction

China's rapid economic growth over the past few decades has led to a dramatic increase in energy demand, particularly in the power sector. China's power system has been dominated by thermal power generation. In 2019, the installed capacity of the thermal power industry in China was 1.19×10^9 kW and it has continued to increase in recent years [1]. The heavy reliance on coal has significant environmental implications, as these plants are major sources of sulfur dioxide (SO_2), nitrogen oxide (NOx), particulate matter (PM), and other pollutants. In 2012, the power sector contributed 33% of NOx, 23% of SO_2, and 8% of PM emissions in China [2]. Beyond their direct effects, emissions from power plants play a crucial role in the formation of secondary pollutants. SO_2, NOx,

and volatile organic compounds (VOCs) serve as precursors to ozone (O_3) and secondary PM components, including sulfate (SO_4^{2-}) and nitrate (NO_3^-). This surge in energy consumption, predominantly met by coal, natural gas, and biomass, has resulted in severe air pollution problems across the country [3,4], and these pollutants pose significant risks to public health [5–9]. Moreover, the effects of power plant emissions are not confined to local areas. Long-range transport of pollutants from East Asia has been observed to impact air quality in regions as distant as the western United States [10,11]. Additionally, PM emissions play a role in climate change by altering the earth's radiation balance and influencing cloud formation processes [12,13].

Recognizing these issues, the Chinese government has implemented stricter emission standards for coal-fired power plants and set ambitious targets to reduce $PM_{2.5}$ levels in major metropolitan areas. In 2011, a new thermal power industry standard (GB13223-2011) replaced the previous standard (GB13223-2003), which was deemed inadequate for effective pollution control [14]. Subsequently, even more stringent "ultra-low emission limits" were introduced nationwide, mandating that emission concentrations of SO_2, NOx, and PM from coal-fired power units must not exceed 35, 50, and 10 mg/m^3, respectively [15]. Despite these efforts and the installation of emission control technologies, challenges persist. While emissions of SO_2 and PM from power generation have shown declining trends, emissions of NOx, CO, CO_2, and VOCs continue to increase [2]. Understanding the impact of power plant emissions on air quality is crucial for developing effective strategies to address this pressing environmental challenge.

Previous studies have employed a variety of methodologies, including receptor models and chemical transport models (CTMs), to investigate the contribution of power generation to air pollution in China [16–19]. In recent years, the environmental impacts of thermal power plant emissions have been extensively studied using various atmospheric chemical transport models in recent years. Chen et al. [20] conducted a comprehensive analysis of thermal power industry emissions in the Fen-Wei Plain of China using the Comprehensive Air Quality Model with extensions (CAMx), providing valuable insights into the regional atmospheric environmental impacts of the thermal power sector. In eastern China, Long et al. [21] employed a two-way coupled air quality model (WRF-Chem) to quantitatively assess the effects of emission reductions from thermal power plants on both air quality and atmospheric temperature. Their findings revealed that such reductions could effectively improve air quality, leading to a significant 10.8% decrease in PM2.5 concentrations. Moreover, they observed that these emission reductions resulted in a decrease of 0.1 W·m^{-2} in the net radiation flux at the top of the atmosphere, highlighting the complex interactions between air pollutants and atmospheric radiation balance. Expanding the geographical scope, Reddington et al. [22] utilized the WRF-Chem regional atmospheric model to investigate the potential air quality and human health benefits of eliminating emissions from six different anthropogenic sectors, including electricity generation, across South and East Asia in 2014. This study provided valuable insights into the broader regional impacts of power plant emissions. In a more focused study on the Beijing–Tianjin–Hebei (BTH) region, Wang et al. [23] employed the Community Multiscale Air Quality (CMAQ) model to evaluate the effectiveness of proposed thermal power plant emission controls. Their simulation results demonstrated that the hypothetical removal of all thermal power plants in the BTH region could lead to substantial reductions in various air pollutants in Beijing, specifically 38% for CO, 23% for both SO_2 and NO_2, and 24% for both PM2.5 and PM10 on an annual mean basis. These findings underscore the significant contribution of thermal power plants to regional air pollution. Furthermore, Wang et al. [24] conducted an innovative study examining the implications of inter-provincial electricity transfer on PM2.5 pollution and associated health and economic losses across mainland China. Their analysis

revealed a notable spatial redistribution of environmental impacts, where the transfer of electricity generation resulted in improved air quality and reduced health burdens in eastern and southern China, but simultaneously led to increased environmental and health impacts in northern, western, and central regions. This study highlighted the importance of considering the geographical redistribution of environmental impacts when implementing energy policies.

However, these investigations have often been limited in scope, focusing on specific regions or time periods, and primarily addressing the impacts on $PM_{2.5}$ and SO_2 concentrations. This approach has left significant gaps in our understanding, particularly concerning the effects on O_3 formation and the broader implications of recently implemented ultra-low emission standards on overall air quality. The limitations of existing research underscore the need for a more comprehensive and up-to-date analysis. Notably, the lack of attention to O_3, a critical secondary pollutant with significant health and environmental impacts, represents a substantial gap in the current literature. Moreover, the rapid evolution of emission control technologies and regulations necessitates a reassessment of power plant emissions' impact on air quality under these new conditions. To address these shortcomings, we employed the Weather Research and Forecast model and Community Multiscale Air Quality (WRF/CMAQ) modeling system to quantify the contribution of power plant emissions to both $PM_{2.5}$ and O_3 levels. The contribution to major secondary components of $PM_{2.5}$ was also investigated. In addition, process analysis was used to examine the impact of power plant emissions on O_3. Individual processes contributing to O_3 concentrations caused by power plant emissions were further assessed. The results of this study will support informed decision-making in energy policy and environmental management, ultimately contributing to the goal of improving air quality and protecting public health in China.

2. Data and Methods

2.1. Model Systems and Data

In this research, we utilized the WRF/CMAQ modeling system to assess the impact of the power sector on air quality in June 2019. Our study employed a nested grid approach: an outer domain covering China (27 km resolution) and an inner domain focusing on the eastern part of China (9 km resolution) (Figure 1).

The WRF model, configured with 35 vertical layers and initialized using NCEP-FNL data [25], generated meteorological inputs. Its physics schemes included: the New Thompson et al. microphysics scheme [26], the Kain–Fritsch cumulus parameterization scheme [27], the rapid radiative transfer model for general circulation models (RRTMG) for short and long wave schemes [28], the Yonsei University (YSU) Planetary Boundary Layer (PBL) physics scheme [29], and the Noah land-surface scheme.

The emissions dataset integrated the Multiresolution Emission Inventory for China (MEIC) [30], biomass burning emissions by Zhou et al. [31], and biogenic sources from MEGANv3.1 (https://bai.ess.uci.edu/megan/resources, accessed on 15 October 2024). MEIC's land-based anthropogenic emissions are from five main sectors, including agriculture, industry, power, residential and transportation.

CMAQ simulations, using the CB06 gas-phase mechanism and AERO7 aerosol module, compared scenarios with and without power emissions to isolate their impact on air quality. We also implemented Integrated Process Rate (IPR) analysis to quantify contributions of various processes to air pollution formation and distribution. The process analysis technique in the CMAQ model is a method designed to quantify and evaluate the contributions of various atmospheric physical and chemical processes to changes in pollutant concentrations. By isolating the effects of individual processes, such as emissions,

chemical reactions, and horizontal transport, this technique provides a detailed understanding of how model predictions are generated and highlights the relative importance of each process. This approach is valuable for identifying potential errors in model formulations or input data, as well as for interpreting differences in model outputs caused by changes in the model or its inputs. Furthermore, chemical process analysis can be used to assess the characteristics of different chemical mechanisms under varying atmospheric conditions, such as VOC- or NOx-limited regimes, offering critical insights for mechanism evaluation and model improvement.

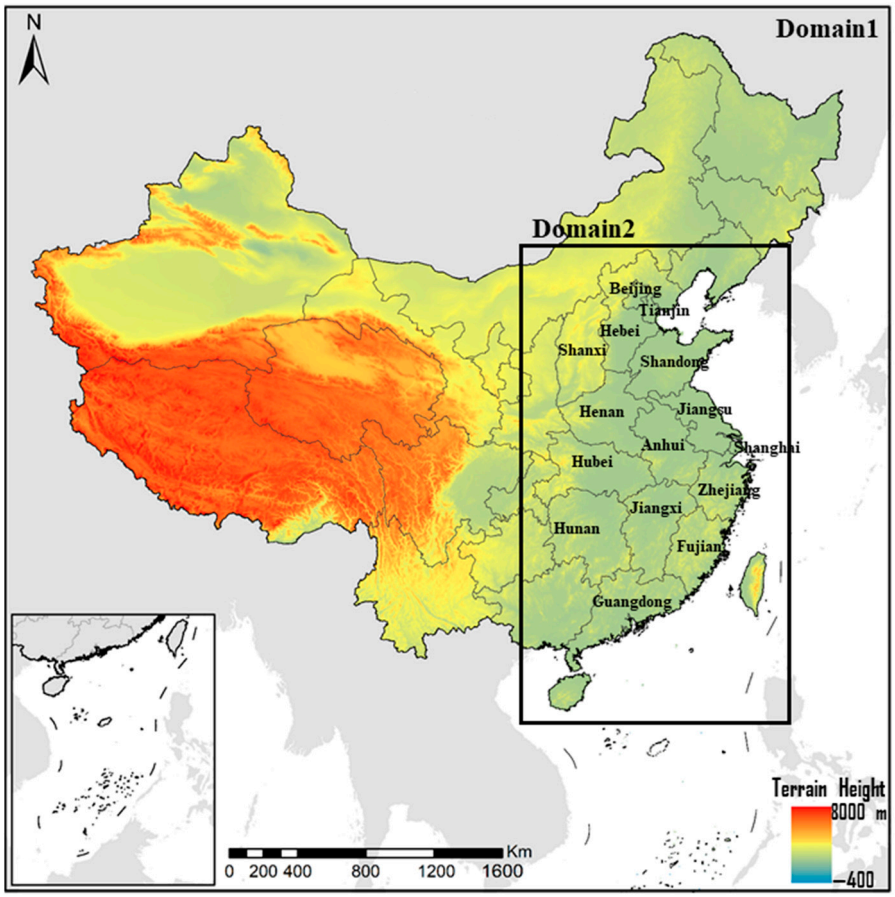

Figure 1. Sketch map of the study area.

2.2. Model Evaluation

In this study, the performance of the WRF and CMAQ models were evaluated for model validation, we conducted a comprehensive comparison between simulated outputs and observational data. The WRF model performance was assessed based on key meteorological parameters, including temperature at 2 m (T_2); relative humidity at 2 m (RH_2); wind speed at 10 m (WS_{10}); and wind direction at 10 m (WD_{10}). Observational data were sourced from 220 available meteorological stations in the study area, provided by the National Climate Data Center. The model's performance was evaluated using a suite of statistical metrics, including mean bias (MB), normalized mean bias (NMB, %), normalized mean error (NME, %), and correlative coefficient (R). The meteorological simulation accuracy was evaluated using criteria established by Emery et al. [32]. Our results indicate that the model's performance meets acceptable standards, with mean biases for T_2, WS_{10}, and WD_{10} falling within the prescribed limits ($\pm$0.5 K, $\pm$0.5 m s^{-1}, and $\pm10^{\circ}$, respectively). Detailed statistical analyses are presented in Table 1.

Table 1. Model performance of meteorological factors.

Parameters	MB [1]	NMB (%) [2]	NME (%) [3]	R [4]
T_2 (°C)	0.4	2.9	7.0	0.9
RH_2 (%)	−3.3	−4.6	11.7	0.9
WS_{10} (m/s)	0.5	26.4	54.0	0.5
WD_{10} (degree)	−9.3	−7.5	37.7	0.4

[1] MB: mean biases; [2] NMB: normalized mean biases; [3] NME, normalized mean errors; [4] R: correlation coefficients.

To further validate the model's capacity to simulate air quality, we compared models and observed hourly concentrations of O_3 and $PM_{2.5}$ at 1120 monitoring sites across the study area. These observational data were obtained from China National Environmental Monitoring Center. In addition to the statistical metrics used in the meteorology evaluation, the mean fractional bias (MFB) and mean fractional error (MFE) were included. As illustrated in Table 2, high correlation coefficients for O_3 and $PM_{2.5}$ indicate good agreement between modeled and measured concentrations. Notably, the statistical metrics align with or surpass the benchmarks established by Boylan and Russell [33] for $PM_{2.5}$, where MFB should not exceed ±60% and MFE should remain within ±75%.

Table 2. Model performance of $PM_{2.5}$ and O_3 concentration.

Parameters	MB [1]	NMB (%) [2]	NME (%) [3]	MFB (%) [4]	MFE (%) [5]	R [6]
$PM_{2.5}$ (μg m^{-3})	0.3	−0.5	64.5	−1.21	61.9	0.6
O_3 (μg m^{-3})	−10.1	−11.1	46.0	−18.0	52.4	0.7

[1] MB: mean biases; [2] NMB: normalized mean biases; [3] NME, normalized mean errors; [4] MFB, mean fractional bias; [5] MFE, mean fractional error; [6] R: correlation coefficients.

This comprehensive evaluation confirms the robustness of our modeling approach, with errors remaining within acceptable ranges. Some discrepancies were noted, primarily attributable to uncertainties in emission inventories and inherent limitations in meteorological and air quality modeling processes.

3. Results

3.1. Emissions from Power Plants

According to the MEIC emission inventory, the emissions of NOx, SO_2 and $PM_{2.5}$ from the power plants in June 2019 were 30.87×10^4, 10.44×10^4 and 1.79×10^4 tons, respectively. Figure 2 illustrates the spatial distribution of these emissions, revealing significant regional heterogeneity. North, East, and South China reflect the dense power demand and thermal power plant distribution. Table 3 further compares power sector emissions with other major anthropogenic sources. While the industrial sector dominates emissions across all pollutants, the power sector's contribution is non-negligible. Notably, in NOx emissions, the power sector contributed 30.87×10^4 tons, second only to the industrial and transportation sectors, accounting for approximately 17.5% of total anthropogenic NOx emissions. For SO_2, power sector emissions of 10.44×10^4 tons represent about 16.7% of the total, ranking second after the industrial sector. Although the power sector's direct contributions to $PM_{2.5}$ and PM_{10} emissions are relatively smaller, the sector's significant emissions of SO_2 and NOx, important precursors to secondary PM formation, suggest a substantial indirect impact on air pollution.

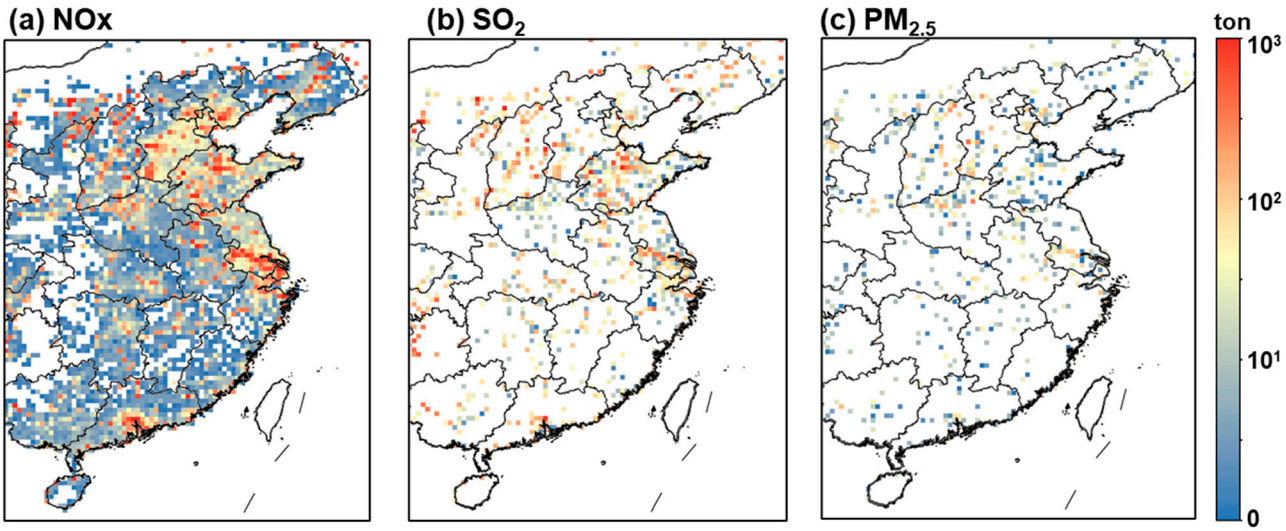

Figure 2. Emissions of air pollutants from power plants in June 2019 (MEIC [30]), (**a**) for NOx emissions, (**b**) for SO_2 emissions and (**c**) for $PM_{2.5}$ emissions.

Table 3. Power plants emissions and other anthropogenic emissions of China in June 2019 (10^4 ton).

	SO_2	NOx	$PM_{2.5}$	PM_{10}
Power	10.44	30.87	1.79	2.79
Industry	39.95	80.41	26.26	39.18
Residential	11.13	3.61	13.40	15.34
Transportation	0.99	61.81	3.66	3.76

3.2. Impact of the Power Plants on Air Quality

Figure 3 illustrates the spatial distribution of the contributions to $PM_{2.5}$ and daily maximum 8 h O_3 concentrations due to power plant emission across eastern China in June. The contribution to $PM_{2.5}$ (Figure 3a) shows a distinct pattern with highest values (2.5–3.0 μg m^{-3}) concentrated in central and eastern regions, particularly in Henan, Anhui, and parts of Shandong. In contrast, coastal areas and southern provinces exhibit lower contributions (<1.0 μg m^{-3}). The O_3 distribution (Figure 3b) presents a more complex pattern, with positive contributions (up to 4 ppb) dominating southern and southeastern coastal regions, while negative values (down to −4 ppb) are observed in the northeast and parts of central China. This inverse relationship in some areas suggests that power plant NOx emissions may lead to O_3 titration in NOx-saturated regions, while contributing to O_3 formation in NOx-limited areas. The transition zones between positive and negative O_3 contributions, particularly evident in central and eastern parts of the domain, highlight the delicate balance in O_3 chemistry and the potential for non-linear responses to emission changes. These areas may be particularly sensitive to shifts in NOx emissions from power plants.

This spatial variability underscores the importance of region-specific strategies in air quality management. While $PM_{2.5}$ reductions from power plant emission controls might be most effective in central and eastern regions, the impacts on O_3 are more complex. In southern coastal areas, NOx reductions could lead to O_3 decreases, whereas in some northern and central regions, the same reductions might potentially increase O_3 levels, at least in the short term.

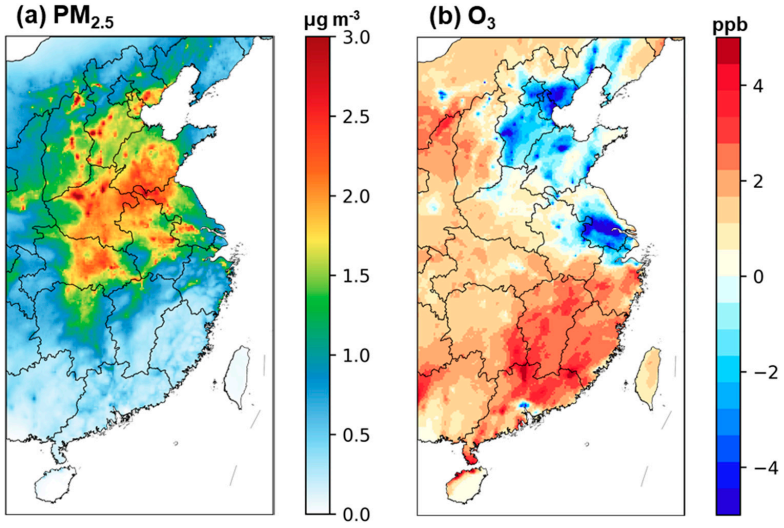

Figure 3. Monthly average contribution of power plant emission. (**a**) Monthly average contribution of power plant emission to $PM_{2.5,}$ and (**b**) monthly average contribution of power plant emission to daily maximum 8 h O_3 in June 2019.

3.3. Impact of the Power Plants on $PM_{2.5}$ Components

The composition of $PM_{2.5}$ can vary significantly even when total mass concentrations are similar. To unravel the complex relationship between emission sources and $PM_{2.5}$ composition, we investigated the contribution of power plant emissions to major secondary components of $PM_{2.5}$, including NO_3^-, SO_4^{2-}, and NH_4^+. As shown in Figure 4, the impact of power plant emissions on these secondary pollutants exhibits distinct patterns and magnitudes.

NO_3^- (Figure 4a) shows the most pronounced contribution, with peak values exceeding 2.0 μg m^{-3} in central and eastern regions, particularly in parts of Henan, Anhui, and Shandong provinces. This pattern likely reflects the significant NOx emissions from coal-fired power plants and subsequent nitrate formation through photochemical processes. The contribution gradually decreases towards coastal and southern areas, with values below 0.5 μg m^{-3}. SO_4^{2-} contributions (Figure 4b) present a more uniform distribution across the region, with most areas showing values between 0.5 and 1.0 μg m^{-3}. This relatively homogeneous pattern may be attributed to the widespread implementation of flue gas desulfurization technologies in power plants, resulting in reduced SO_2 emissions and subsequent sulfate formation. NH_4^+ contributions (Figure 4c) exhibit a spatial pattern similar to that of SO_4^{2-}, but with slightly lower magnitudes, generally below 0.5 μg m^{-3} across most of the domain. The contrasting spatial patterns among these secondary components highlight the complex interplay between power plant emissions, atmospheric chemistry, and regional transport processes. The significantly higher contribution to NO_3^- compared to SO_4^{2-} and NH_4^+ suggests that NOx emissions from power plants play a dominant role in secondary $PM_{2.5}$ formation in this region during the study period. These findings underscore the importance of targeted emission control strategies, particularly for NOx, in mitigating the impact of power plant emissions on regional air quality.

3.4. Diurnal Impact of the Power Plants on O_3

The temporal dynamics of O_3 formation are driven by complex photochemical processes that vary throughout the day, influenced by factors such as solar radiation, temperature, and precursor emissions. To elucidate these processes, we analyzed the hourly changes in O_3 concentrations attributable to power plant emissions across eastern China. Figure 5 illustrates the diurnal variation of O_3 concentration changes due to power plant

emissions at four time points: 8:00, 12:00, 16:00, and 20:00 local time (LT), revealing distinct spatiotemporal patterns. At 8:00 LT (Figure 5a), negative O_3 changes (up to −4 ppb) dominate most of the region, particularly in the northeast and central areas, indicating O_3 titration by NOx emissions from power plants. As the solar radiation intensifies, positive O_3 changes emerge and strengthen, especially in the southern and coastal regions. By 12:00 LT (Figure 5b), a clear north–south divide becomes evident, with persistent negative changes in the northeast contrasting with increasing positive changes (up to 4 ppb) in the south. The positive O_3 contribution due to power plant emission peaks at 16:00 LT (Figure 5c), with extensive areas in the south and southeast experiencing increases of over 4 ppb, likely due to enhanced photochemical reactions. By 20:00 LT (Figure 5d), the positive O_3 changes begin to diminish, though they remain significant in the southern regions. Throughout the day, the northeast consistently shows negative O_3 changes, suggesting a NOx-saturated regime where power plant emissions suppress O_3 formation.

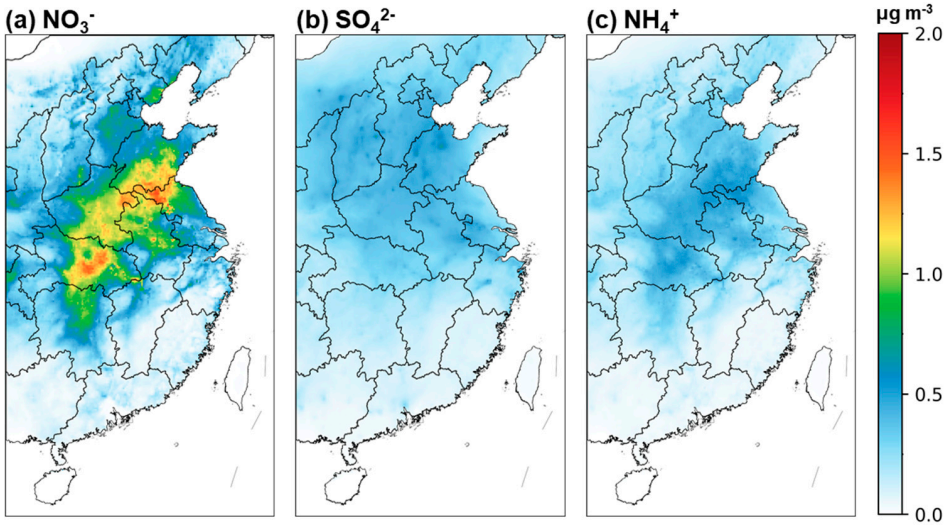

Figure 4. Contribution of power plant emission to the concentration of secondary components of $PM_{2.5}$, including (**a**) contribution of power plant emission to the concentration of NO_3^-, (**b**) contribution of power plant emission to the concentration of SO_4^{2-} and (**c**) contribution of power plant emission to the concentration of NH_4^+ in June 2019.

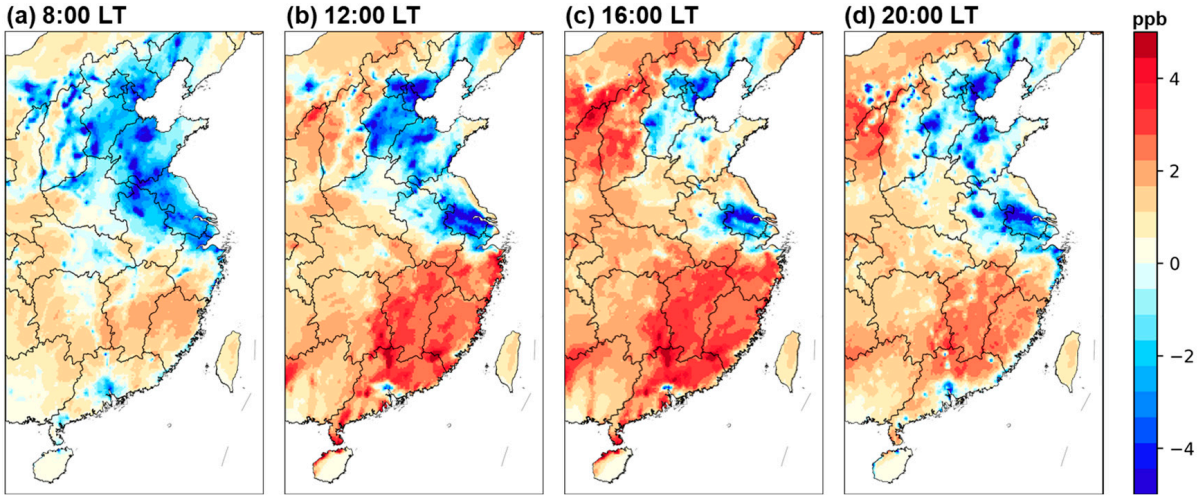

Figure 5. Monthly average diurnal variation of O_3 concentration due to power plant emissions at four time points: (**a**) for morning (8:00), (**b**) for noon (12:00), (**c**) for afternoon (16:00), and (**d**) for evening (20:00) local time (LT).

3.5. Process Analysis of Power Plant Impacts on O_3

Given the pronounced impact of power plant emissions on O_3 concentrations at 16:00 LT, we conducted a detailed analysis of the contributions from various atmospheric processes. Figure 6 illustrates the process-specific contributions to surface O_3 concentrations due to power plant emissions at 16:00 LT, as simulated using the Process Analysis (PA) module in the CMAQ model.

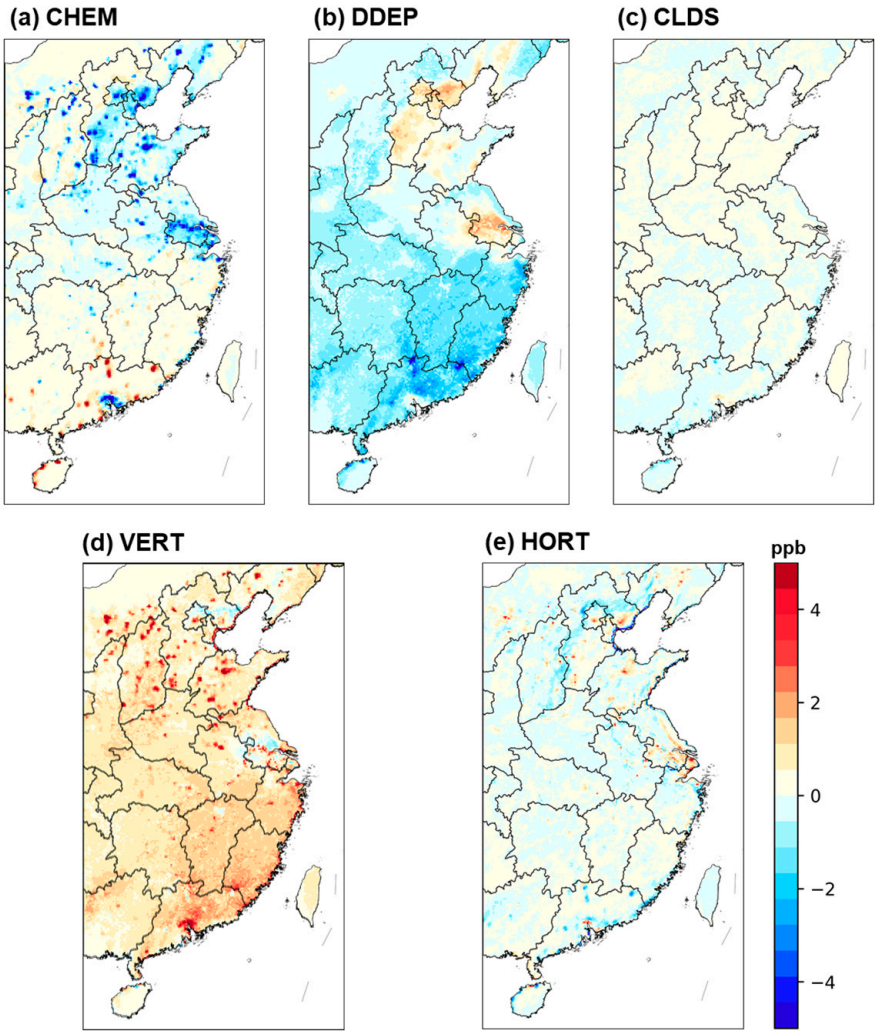

Figure 6. Average process contributions to O_3 due to power plant emissions at surface layer at 16:00 LT. (**a**) for chemical process contributions to O_3, (**b**) for dry deposition contributions to O_3, (**c**) for cloud processes contributions to O_3, (**d**) for vertical transport processes contributions to O_3, and (**e**) for horizontal transport for processes contributions to O_3.

The chemical process (CHEM, Figure 6a) exhibits a complex spatial distribution. Negative contributions (blue areas) dominate in most coastal regions and some inland areas, suggesting O_3 depletion due to power plant emissions, likely attributed to the NOx titration effect in NOx-rich environments [34–36]. Conversely, positive contributions (red areas) are observed in southern coastal and certain inland locations, indicating that power plant emissions promote net O_3 production, possibly due to optimal VOCs/NOx ratios for O_3 formation in these areas. Dry deposition (DDEP, Figure 6b) predominantly shows negative contributions across the domain, particularly pronounced in the southeastern coastal areas. This indicates that a significant portion of O_3 produced or influenced by power plant emissions is removed through dry deposition. Cloud processes (CLDS, Figure 6c) demonstrate minimal impact on O_3 concentrations derived from power plant emissions, with most areas

showing near-neutral effects. This suggests that during the study period, cloud interactions had little influence on the fate of O_3 produced from power plant emissions. Vertical transport (VERT, Figure 6d) emerges as the dominant positive contributor, with significant positive values across almost the entire study area. This indicates substantial downward mixing of O_3 or its precursors originating from power plant emissions at higher altitudes, enhancing surface O_3 concentrations. The effect is particularly pronounced in coastal regions and certain inland areas, possibly due to the interaction between power plant plume heights and local atmospheric dynamics. Horizontal transport (HORT, Figure 6e) presents a complex spatial pattern with both positive and negative contributions. Negative contributions in coastal areas suggest that O_3, or its precursors from power plants, are being transported away from these regions. Positive contributions in some inland areas, particularly around major urban clusters, likely indicate the regional transport of power plant-derived O_3 or its precursors into these areas.

These results reveal the intricate mechanisms by which power plant emissions influence O_3 concentrations through various atmospheric processes. Vertical transport emerges as the primary process increasing surface O_3 levels from power plant emissions, while dry deposition acts as the main removal mechanism. The roles of chemical processes and horizontal transport vary spatially, reflecting the complex interactions between power plant emissions, local atmospheric conditions, and regional transport patterns.

4. Conclusions

This study employed the WRF/CMAQ modeling system to quantify the contribution of power plant emissions to $PM_{2.5}$ and O_3 levels across eastern China in June 2019, with a focus on secondary $PM_{2.5}$ components and process-specific contributions to O_3 formation. Our comprehensive analysis reveals complex spatial and temporal patterns in the impact of power plant emissions on regional air quality. Our findings demonstrate that power plant emissions significantly influence $PM_{2.5}$ concentrations, with the most pronounced effects observed in central and eastern regions, where contributions reach 2.5–3.0 μg m^{-3}. The impact on O_3 exhibits a more intricate distribution, characterized by positive contributions (up to 4 ppb) in southern and southeastern coastal regions and negative values (down to −4 ppb) in the northeast and parts of central China. This pattern underscores the nuanced relationship between power plant NOx emissions and O_3 formation, reflecting varying NOx saturation levels across the region. Analysis of secondary $PM_{2.5}$ components reveals that power plant emissions contribute most significantly to NO_3^- formation, with smaller impacts on SO_4^{2-} and NH_4^+. This finding highlights the critical role of NOx emissions in secondary $PM_{2.5}$ formation and emphasizes the need for targeted NOx control strategies in the power sector. The diurnal analysis of O_3 changes due to power plant emissions uncovers a complex spatiotemporal pattern. We observe a transition from widespread O_3 suppression in the early morning to significant O_3 enhancement in southern regions during peak sunlight hours, while the northeast consistently exhibits O_3 reduction. This temporal variability underscores the region-specific and time-dependent nature of power plant emissions' impact on O_3 formation. Process-specific analysis at 16:00 LT reveals that vertical transport is the dominant mechanism enhancing surface O_3 levels from power plant emissions, while dry deposition acts as the primary removal process.

This study provides insights into the role of power plant emissions in shaping regional air quality, which has significant implications for sustainable development. By quantifying the contributions of power plant emissions to $PM_{2.5}$ and O_3 levels, our findings highlight the critical need for targeted emission control strategies, particularly focusing on NOx reductions, to mitigate air pollution and its associated health and environmental impacts. These results support the development of region-specific air quality management policies

that balance economic growth with environmental protection, aligning with the principles of sustainable development. Furthermore, the study underscores the importance of integrating advanced modeling tools, such as WRF/CMAQ, into sustainability planning to better understand the complex interactions between industrial emissions and atmospheric chemistry. By addressing the environmental challenges posed by the thermal power industry, this research contributes to the broader goal of achieving cleaner air, healthier ecosystems, and improved quality of life, which are essential components of a sustainable future.

Author Contributions: Conceptualization, X.Z. and W.T.; methodology, X.Z., W.T. and D.C.; validation, W.T. and D.C.; formal analysis, X.Z. and D.C.; data curation, X.Z.; writing—original draft preparation, X.Z.; writing—review and editing, X.Z., W.T. and D.C.; visualization, X.Z. and W.T.; supervision, W.T. and D.C.; project administration, D.C.; funding acquisition, D.C. All authors have read and agreed to the published version of the manuscript.

Funding: This research was funded by the Opening Project of State Key Laboratory of Low-carbon Smart Coal-fired Power Generation and Ultra-clean Emission (D2022FK082).

Institutional Review Board Statement: Not applicable.

Informed Consent Statement: Not applicable.

Data Availability Statement: The data presented in this study are openly available in the references [25,30].

Acknowledgments: This paper represents the perspectives of the authors and does not necessarily represent the official views of our sponsors. We would like to thank the anonymous reviewers for their valuable comments and suggestions to improve the manuscript.

Conflicts of Interest: Authors Xiuyong Zhao and Wenxin Tian were employed by the company China Energy Science and Technology Research Institute Co., Ltd. The remaining authors declare that the research was conducted in the absence of any commercial or financial relationships that could be construed as a potential conflict of interest.

References

1. China Statistical Yearbook. Available online: https://www.stats.gov.cn/sj/ndsj/2023/indexch.htm (accessed on 15 October 2024).
2. Huang, L.; Hu, J.; Chen, M.; Zhang, H. Impacts of power generation on air quality in China—Part I: An overview. *Resour. Conserv. Recycl.* **2017**, *121*, 103–114. [CrossRef]
3. Chan, C.K.; Yao, X. Air pollution in mega cities in China. *Atmos. Environ.* **2008**, *42*, 1–42. [CrossRef]
4. Hu, J.; Wang, Y.; Ying, Q.; Zhang, H. Spatial and temporal variability of PM2.5 and PM10 over the North China Plain and the Yangtze River Delta, China. *Atmos. Environ.* **2014**, *95*, 598–609. [CrossRef]
5. Anenberg, S.C.; Horowitz, L.W.; Tong, D.Q.; West, J.J. An estimate of the global burden of anthropogenic ozone and fine particulate matter on premature human mortality using atmospheric modeling. *Environ. Health Perspect.* **2010**, *118*, 1189–1195. [CrossRef] [PubMed]
6. Chen, B.; Kan, H.; Chen, R.; Jiang, S.; Hong, C. Air Pollution and Health Studies in China—Policy Implications. *J. Air Waste Manag. Assoc.* **2011**, *61*, 1292–1299. [CrossRef] [PubMed]
7. Kan, H.; London, S.J.; Chen, G.; Zhang, Y.; Song, G.; Zhao, N.; Jiang, L.; Chen, B. Season, sex, age, and education as modifiers of the effects of outdoor air pollution on daily mortality in Shanghai, China: The Public Health and Air Pollution in Asia (PAPA) study. *Environ. Health Perspect.* **2008**, *116*, 1183–1188. [CrossRef] [PubMed]
8. Laurent, O.; Hu, J.; Li, L.; Cockburn, M.; Escobedo, L.; Kleeman, M.J.; Wu, J. Sources and contents of air pollution affecting term low birth weight in Los Angeles County, California, 2001–2008. *Environ. Res.* **2014**, *134*, 488–495. [CrossRef] [PubMed]
9. Pope Iii, C.A. Review: Epidemiological basis for particulate air pollution health standards. *Aerosol Sci. Technol.* **2000**, *32*, 4–14. [CrossRef]
10. Wang, K.C.; Chin, C.L.; Tsai, Y.H. A wavelet-based denoising system using time-frequency adaptation for speech enhancement. In Proceedings of the 2009 International Conference on Asian Language Processing: Recent Advances in Asian Language Processing, IALP 2009, Singapore, 7–9 December 2009; pp. 114–117.

11. Ying, Q.; Wu, L.; Zhang, H. Local and inter-regional contributions to PM2.5 nitrate and sulfate in China. *Atmos. Environ.* **2014**, *94*, 582–592. [CrossRef]
12. Fan, J.; Leung, L.R.; Demott, P.J.; Comstock, J.M.; Singh, B.; Rosenfeld, D.; Tomlinson, J.M.; White, A.; Prather, K.A.; Minnis, P.; et al. Erratum: Aerosol impacts on California winter clouds and precipitation during CalWater 2011: Local pollution versus long-range transported dust published in (Atmospheric Chemistry and Physics (2014) 14 (81-101)). *Atmos. Chem. Phys.* **2014**, *14*, 3063–3064. [CrossRef]
13. Wang, Y.; Wang, M.; Zhang, R.; Ghan, S.J.; Lin, Y.; Hu, J.; Pan, B.; Levy, M.; Jiang, J.H.; Molina, M.J. Assessing the effects of anthropogenic aerosols on Pacific storm track using a multiscale global climate model. *Proc. Natl. Acad. Sci. USA* **2014**, *111*, 6894–6899. [CrossRef]
14. Emission Standard of Air Pollutants for Thermal Power Plants. Available online: https://www.mee.gov.cn/ywgz/fgbz/bz/bzwb/dqhjbh/dqgdwrywrwpfbz/201109/t20110921_217534.shtml (accessed on 15 October 2024).
15. Upgrade and Retrofit Plan for Coal-Fired Power Plants Aiming at Energy Savings and Emissions Reduction for 2014–2020. Available online: https://www.gov.cn/gongbao/content/2015/content_2818468.htm (accessed on 15 October 2024).
16. Zhang, R.; Jing, J.; Tao, J.; Hsu, S.C.; Wang, G.; Cao, J.; Lee, C.S.L.; Zhu, L.; Chen, Z.; Zhao, Y.; et al. Chemical characterization and source apportionment of PM2.5 in Beijing: Seasonal perspective. *Atmos. Chem. Phys.* **2013**, *13*, 7053–7074. [CrossRef]
17. Tao, J.; Gao, J.; Zhang, L.; Zhang, R.; Che, H.; Zhang, Z.; Lin, Z.; Jing, J.; Cao, J.; Hsu, S.C. PM2.5 pollution in a megacity of southwest China: Source apportionment and implication. *Atmos. Chem. Phys.* **2014**, *14*, 8679–8699. [CrossRef]
18. Wang, D.; Hu, J.; Xu, Y.; Lv, D.; Xie, X.; Kleeman, M.; Xing, J.; Zhang, H.; Ying, Q. Source contributions to primary and secondary inorganic particulate matter during a severe wintertime PM2.5 pollution episode in Xi'an, China. *Atmos. Environ.* **2014**, *97*, 182–194. [CrossRef]
19. Zhang, Y.; Bo, X.; Zhao, Y.; Nielsen, C.P. Benefits of current and future policies on emissions of China's coal-fired power sector indicated by continuous emission monitoring. *Environ. Pollut.* **2019**, *251*, 415–424. [CrossRef]
20. Chen, L.; Wang, T.; Bo, X.; Zhuang, Z.; Qu, J.B.; Xue, X.D.; Tian, J.; Huang, M.T.; Wang, P.; Sang, M.J. Thermal Power Industry Emissions and Their Contribution to Air Quality on the Fen-Wei Plain. *Atmosphere* **2022**, *13*, 652. [CrossRef]
21. Long, Z.-Y.; Zhu, J.; Li, K.; Chen, L.; Du, N.; Liao, H. [Impact of Emission Reduction in Different Sectors on Air Quality and Atmospheric Temperature in Eastern China]. *Huanjing kexue* **2023**, *44*, 5889–5898. [CrossRef]
22. Reddington, C.L.; Conibear, L.; Knote, C.; Silver, B.; Li, Y.J.; Chan, C.K.; Arnold, S.R.; Spracklen, D.V. Exploring the impacts of anthropogenic emission sectors on $PM_{2.5}$ and human health in South and East Asia. *Atmos. Chem. Phys.* **2019**, *19*, 11887–11910. [CrossRef]
23. Wang, L.Q.; Li, P.F.; Yu, S.C.; Mehmood, K.; Li, Z.; Chang, S.C.; Liu, W.P.; Rosenfeld, D.; Flagan, R.C.; Seinfeld, J.H. Predicted impact of thermal power generation emission control measures in the Beijing-Tianjin-Hebei region on air pollution over Beijing, China. *Sci. Rep.* **2018**, *8*, 934. [CrossRef] [PubMed]
24. Wang, J.X.; Zhou, S.; Huang, T.; Ling, Z.L.; Liu, Y.; Song, S.J.; Ren, J.; Zhang, M.L.; Yang, Z.L.; Wei, Z.J.; et al. Air pollution and associated health impact and economic loss embodied in inter-provincial electricity transfer in China. *Sci. Total Environ.* **2023**, *883*, 163653. [CrossRef] [PubMed]
25. NCEP. Available online: https://rda.ucar.edu/datasets/ds083.2/ (accessed on 15 October 2024).
26. Thompson, G.; Field, P.R.; Rasmussen, R.M.; Hall, W.D. Explicit Forecasts of Winter Precipitation Using an Improved Bulk Microphysics Scheme. Part II: Implementation of a New Snow Parameterization. *Mon. Weather. Rev.* **2008**, *136*, 5095–5115. [CrossRef]
27. Kain, J.S. The Kain–Fritsch Convective Parameterization: An Update. *J. Appl. Meteorol.* **2004**, *43*, 170–181. [CrossRef]
28. Iacono, M.J.; Delamere, J.S.; Mlawer, E.J.; Shephard, M.W.; Clough, S.A.; Collins, W.D. Radiative forcing by long-lived greenhouse gases: Calculations with the AER radiative transfer models. *J. Geophys. Res. Atmos.* **2008**, *113*, D13103. [CrossRef]
29. Hong, S.-Y.; Noh, Y.; Dudhia, J. A New Vertical Diffusion Package with an Explicit Treatment of Entrainment Processes. *Mon. Weather. Rev.* **2006**, *134*, 2318–2341. [CrossRef]
30. MEIC. Available online: http://www.meicmodel.org/ (accessed on 15 October 2024).
31. Zhou, Y.; Xing, X.; Lang, J.; Chen, D.; Cheng, S.; Wei, L.; Wei, X.; Liu, C. A comprehensive biomass burning emission inventory with high spatial and temporal resolution in China. *Atmos. Chem. Phys.* **2017**, *17*, 2839–2864. [CrossRef]
32. Emery, C.; Tai, E. Enhanced Meteorological Modeling and Performance Evaluation for Two Texas Ozone Episodes. Available online: https://www.semanticscholar.org/paper/Enhanced-Meteorological-Modeling-and-Performance-Emery-Tai/3faa521b77acb7158769d9523be8f33e1d7e7ec6 (accessed on 15 October 2024).
33. Boylan, J.W.; Russell, A.G. PM and light extinction model performance metrics, goals, and criteria for three-dimensional air quality models. *Atmos. Environ.* **2006**, *40*, 4946–4959. [CrossRef]
34. Ren, J.; Guo, F.F.; Xie, S.D. Diagnosing ozone-NO_x-VOC sensitivity and revealing causes of ozoneincreases in China based on 2013-2021 satellite retrievals. *Atmos. Chem. Phys.* **2022**, *22*, 15035–15047. [CrossRef]

35. Zhao, M.; Zhang, Y.N.; Pei, C.L.; Chen, T.S.; Mu, J.S.; Liu, Y.H.; Wang, Y.J.; Wang, W.X.; Xue, L.K. Worsening ozone air pollution with reduced NOx and VOCs in the Pearl River Delta region in autumn 2019: Implications for national control policy in China. *J. Environ. Manag.* **2022**, *324*, 116327. [CrossRef]
36. Wang, Y.; Yaluk, E.A.; Chen, H.; Jiang, S.; Huang, L.; Zhu, A.; Xiao, S.; Xue, J.; Lu, G.; Bian, J.; et al. The Importance of NO_x Control for Peak Ozone Mitigation Based on a Sensitivity Study Using CMAQ-HDDM-3D Model During a Typical Episode Over the Yangtze River Delta Region, China. *J. Geophys. Res. Atmos.* **2022**, *127*, e2022JD036555. [CrossRef]